

Title: Three-Dimensional Electronic Scaffolds for Monitoring and Regulation of Multifunctional Hybrid Tissues

Xueju Wang[†], Ron Feiner[†], Haiwen Luan[†], Qihui Zhang, Shiwei Zhao, Yi Zhang, Mengdi Han, Yi Li, Rujie Sun, Heling Wang, Tzu-Li Liu, Xiaogang Guo, Hadas Oved, Nadav Noor, Assaf Shapira, Yihui Zhang, Yonggang Huang, Tal Dvir*, and John A. Rogers**

[*] Prof. John A. Rogers, Corresponding-Author
Department of Materials Science and Engineering, Biomedical Engineering, Neurological Surgery, Chemistry, Mechanical Engineering, Electrical Engineering and Computer Science
Simpson Querrey Institute and Feinberg Medical School
Center for Bio-Integrated Electronics
Northwestern University
Evanston, Illinois 60208 (USA)
E-mail: jrogers@northwestern.edu

[*] Prof. Tal Dvir, Corresponding-Author
School for Molecular Cell Biology and Biotechnology; The Center for Nanoscience and Nanotechnology; Department of Materials Science and Engineering; Sagol Center for Regenerative medicine
Tel Aviv University
Tel Aviv, 69978 (Israel)
Email: tdvir@post.tau.ac.il

[*] Prof. Yonggang Huang, Corresponding-Author
Departments of Mechanical Engineering, Civil and Environmental Engineering, and Materials Science and Engineering; Center for Bio-Integrated Electronics
Northwestern University
Evanston, IL 60208 (USA)
Email: y-huang@northwestern.edu

Prof. Xueju Wang
Department of Mechanical and Aerospace Engineering, University of Missouri, Columbia, MO 65211, USA

Dr. Ron Feiner
School for Molecular Cell Biology and Biotechnology; The Center for Nanoscience and Nanotechnology, Tel Aviv University, Tel Aviv, 69978, Israel

Dr. Haiwen Luan
Departments of Mechanical Engineering, Civil and Environmental Engineering, and Materials Science and Engineering; Center for Bio-Integrated Electronics, Northwestern University
Evanston, Illinois 60208, USA

Mr. Qihui Zhang
Simpson Querrey Institute and Feinberg Medical School; Center for Bio-Integrated Electronics, Northwestern University, Evanston, Illinois 60208, USA

Mr. Shiwei Zhao
Departments of Civil and Environmental Engineering, Mechanical Engineering, and Materials Science and Engineering, Northwestern University, Evanston, Illinois 60208, USA.

School of Aeronautic Science and Engineering, Beihang University, Beijing 100191, P.R. China

Prof. Yi Zhang
Department of Biomedical, Biological, and Chemical Engineering, University of Missouri, Columbia, MO 65211, USA

Dr. Mengdi Han
Simpson Querrey Institute and Feinberg Medical School; Center for Bio-Integrated Electronics, Northwestern University, Evanston, Illinois 60208, USA

Mr. Yi Li
Department of Mechanical and Aerospace Engineering, University of Missouri, Columbia, MO 65211, USA

Dr. Rujie Sun
Department of Materials, Department of Bioengineering and Institute of Biomedical Engineering, Imperial College London, Prince Consort Road, London SW7 2AZ, UK

Dr. Heling Wang
Departments of Civil and Environmental Engineering, Mechanical Engineering, and Materials Science and Engineering, Northwestern University, Evanston, Illinois 60208, USA.

Mr. Tzu-Li Liu
Departments of Mechanical Engineering, Northwestern University, Evanston, Illinois 60208, USA

Dr. Xiaogang Guo
Institute of Advanced Structure Technology, Beijing Institute of Technology, Beijing, 100081, P.R. China

Ms. Hadas Oved
School for Molecular Cell Biology and Biotechnology
Tel Aviv University, Tel Aviv, 69978, Israel

Mr. Nadav Noor
School for Molecular Cell Biology and Biotechnology
Tel Aviv University, Tel Aviv, 69978, Israel

Dr. Assaf Shapira
School for Molecular Cell Biology and Biotechnology
Tel Aviv University, Tel Aviv, 69978, Israel

Prof. Yihui Zhang
Center for Flexible Electronics Technology; Applied Mechanics Laboratory, Department of Engineering Mechanics, Tsinghua University, Beijing 100084, P.R. China

† These authors contributed equally to this work

Keywords: 3D electronic scaffolds, cardiac tissue engineering, electronic stimulation, drug release, mechanically-guided assembly

Abstract

Recently, the integration of electronic elements with cellular scaffolds has brought forth the ability to monitor and control tissue function actively by using flexible free-standing two-dimensional (2D) systems. Capabilities for electrically probing complex, physicochemical and biological three-dimensional (3D) microenvironments demand, however, 3D electronic scaffolds with well-controlled geometries and functional-component distributions. This work presents the development of flexible 3D electronic scaffolds with precisely defined dimensions and microelectrode configurations formed using a process that relies on geometric transformation of 2D precursors by compressive buckling. It demonstrates a capability to fabricate these constructs in diverse 3D architectures and/or electrode distributions aimed at achieving an enhanced level of control and regulation of tissue function relatively to that of other approaches. In addition, this work presents the integration of these 3D electronic scaffolds within engineered 3D cardiac tissues, for monitoring of tissue function, controlling tissue contraction through electrical stimulation, and initiating on-demand, local release of drugs, each through well-defined volumetric spaces. These ideas provide opportunities in fields ranging from in vitro drug development to in vivo tissue repair and many others.

1. Introduction

Since its emergence in the 1980s, tissue engineering has evolved as an interdisciplinary field aimed at developing biological substitutes by combining cells with highly porous three-dimensional (3D) scaffold biomaterials to repair, replace, or regenerate damaged tissues.¹⁻⁴ The scaffolds, which are analogous in function to the extracellular matrix (ECM) in native tissues, act as templates for cell attachment and tissue regeneration, representing a key component of engineered tissues.^{5,6} A variety of biomaterials and fabrication techniques has been used to manufacture scaffolds in attempts to repair and regenerate different tissues and organs in the body. However, capabilities for localized real-time monitoring of cellular activities and physicochemical change represent longstanding needs in the development of scaffolds for regulating and tracking the behaviors of cells throughout their 3D micro-environment.

Recent work demonstrates the use of planar electronic sensors to probe neuronal^{7,8} and electrical activities near natural tissue surfaces including those of the heart,⁹⁻¹² brain¹³ and skin.¹⁴⁻¹⁶ Capabilities in electrically probing the physicochemical and biological microenvironments throughout their 3D and macroporous interior demand, however, a seamless 3D integration of electronics with biomaterials and tissues. Several recent publications report the integration of flexible electronic sensors with 3D porous scaffolds for online monitoring and regulation of engineered cardiac, neuronal, and muscle tissue function.¹⁷⁻²⁰ These hybrid electronic-tissue systems include silicon nanowire field-effect-transistor (FET)-based nanoelectronic scaffolds fabricated by self-organization or folding of planar networks,^{19,20} and multi-microelectrode-based electronic scaffolds by folding of two-dimensional (2D) patches.¹⁸ Such scaffolds can provide real-time monitoring of local electrical activities within 3D electronic/tissue constructs.^{18,20,21} Electrical stimulation at specific locations enables integrated cardiac tissues to be paced online, as well as drug and biofactor release from designated electroactive polymer deposition for the regulation of tissue function.

More recent studies illustrate the ability to fabricate such devices using biodegradable polymers in a manner that allows control over the lifetime of the implanted electronic components.¹⁷ Although such collective approaches to the integration of electronics within engineered tissues create many exciting possibilities in biological research, several challenges remain. For example, the folding processes used to produce these 3D electronic scaffolds can interfere with the formation of a continuous, thick, engineered tissue and thus reduce its sustainable thickness and overall function. In addition, with existing technologies, it is very difficult to precisely control the 3D locations and/or spatial distributions of electrodes for accurate and designated electrical monitoring and regulation of 3D tissue function.

In this work, we report on the development of 3D porous, flexible electronic scaffolds with well-defined microelectrode distributions and we demonstrate their integration with engineered cardiac tissues as a proof of principle, for the sensing, stimulation and regulation of tissue function. These 3D electronic scaffolds are formed by compressive buckling of strategically designed 2D precursor structures, in an overall process of controlled, geometric transformation that offers the ability to realize a diverse array of architectures and configurations in nearly any class of materials, with dimensions ranging from nanometer to centimeter length scales.²²⁻³⁰ The porous nature of these constructs allows for integration within thermoresponsive extracellular matrix (ECM)-based hydrogels that serve as structural supports for cardiac cell seeding and tissue organization. Programmed drug release can occur from within electroactive polymers integrated directly into this framework. Extracellular potential recordings are possible from electrodes with well-controlled locations within the tissue, as well as stimulation by other designated electrodes. The development of such 3D hybrid electronic-tissue interfaces could provide a new avenue for regenerative medicine, pharmacology and electronic therapeutics.

2. Results and Discussions

2.1 Mechanics-guided assembly of 3D electronic scaffolds

Figure 1 shows a schematic illustration of the main fabrication steps, in an overall process that follows published reports.^{22,23,28,30} The scheme begins with the microfabrication of a 2D precursor consisting of patterned thin films of polyimide (PI, 6 μm) and gold (300 nm) on a planar substrate by photolithography and metal etching (Figure S1 and S2, Supporting Information). Transfer of the 2D structure onto the surface of a water-soluble tape (polyvinyl alcohol; 3M Co.) is followed by the spatially selective deposition of a thin layer of Ti (5 nm) and SiO₂ (50 nm) at certain locations to yield surface hydroxyl termination after exposure to ozone. These sites of activated bilayers of Ti/SiO₂ form strong, selective bonds through condensation reactions upon transfer onto a prestrained silicone elastomer substrate (Dragon Skin 10 Slow; Smooth-On, Inc., Easton, PA), also functionalized with surface hydroxyl groups by blanket exposure to ozone. The interfacial interactions at all other locations are dominated by comparatively weak van der Waals forces. Releasing the prestrain in the elastomer induces large compressive forces on the 2D structure at the bonding sites and creates a targeted 3D architecture deterministically by compressive buckling (Figure S3 and Movie S1, Methods, Supporting Information).

This mechanics-guided 3D assembly technique allows for precise control of the dimensions of the resulting 3D electronic scaffolds, including the spatial distribution of microelectrodes for sensing, stimulation, and regulation of tissue function. These microelectrodes consist of gold thin films encapsulated within two layers of PI, the top one of which has the same geometry as

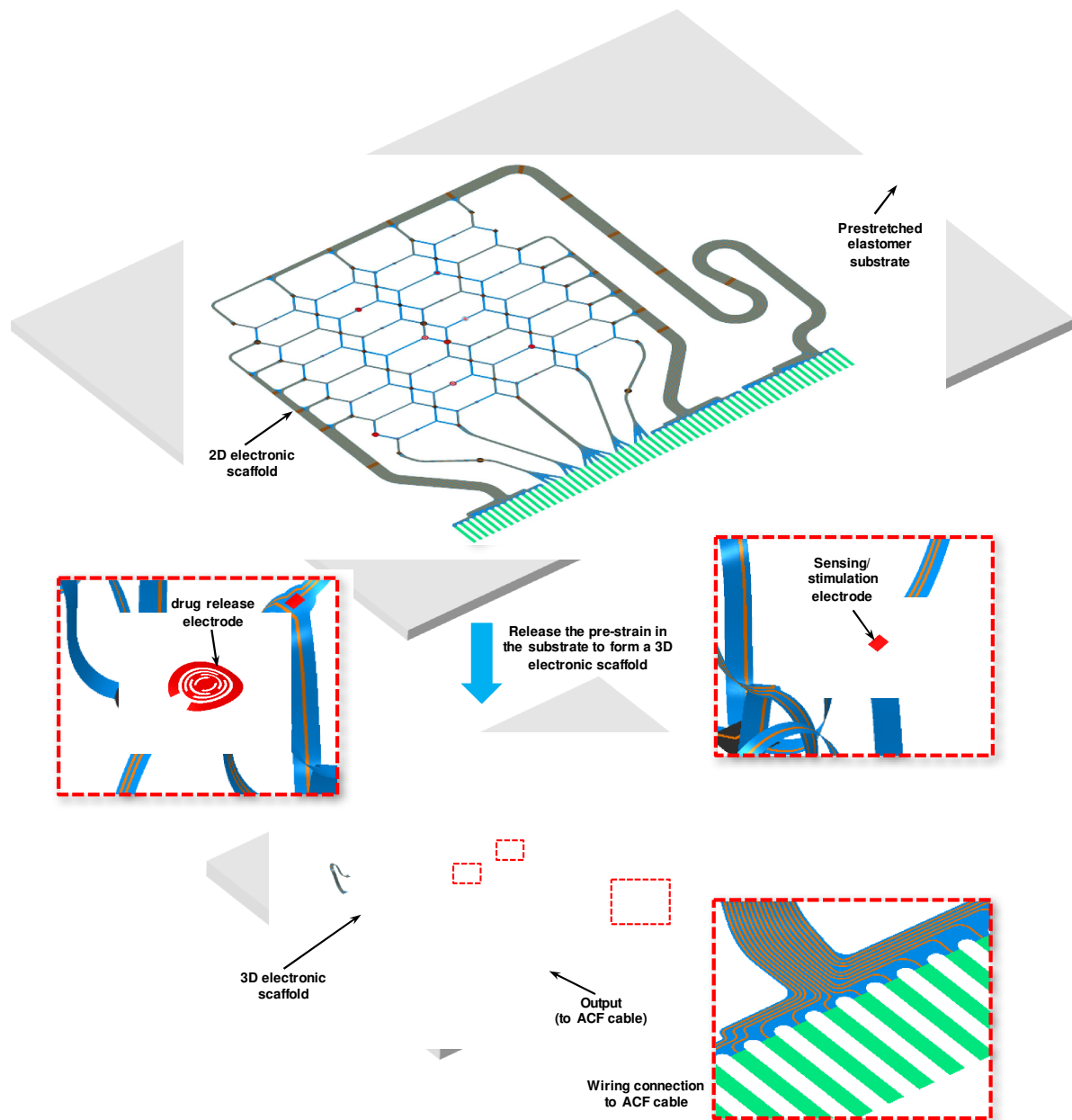


Figure 1. Schematic illustrations of the assembly schemes and layouts for 3D electronic tissue scaffolds. The scaffold forms through a well-controlled, mechanically-guided assembly approach that geometrically transforms a 2D precursor structure into a 3D layout. The resulting flexible, open-network 3D electronic devices include electrodes for electrical sensing, stimulation of cells and tissues, and for drug release.

the bottom, except for the square/circular openings to expose the underlying gold. As shown in the magnified views in Figure 1, microscale square gold pads (50 μm in side length, 300 nm in thickness) patterned at multiple locations across the 3D scaffolds allow noninvasive recordings of cellular electrical activities and electrical stimulation for synchronizing cell contraction. Submillimeter circular electrodes (400 μm in diameter) serve as platforms for the deposition of

drug-contained electroactive polymers to allow for on-demand, controlled release of drugs to regulate the function of engineered tissues, as will be discussed in detail subsequently. Flexible interconnects formed at contact pads at the periphery of the system (illustrated in green in Figure 1) enable interfaces to external electronics for data acquisition and power input using anisotropic conductive film (ACF) cables. The electronic network is thin (6 μm) and highly porous to facilitate matrix and cell infiltration, thereby ensuring minimal interference with the engineered tissue. Compared with existing electronic scaffolds¹⁸⁻²⁰ that rely on flexible 2D systems, the 3D electronic scaffolds introduced here allow the investigation of tissue assembly in all three dimensions without any additional manipulation, as a versatile avenue for the evaluation and regulation of engineered tissues in 3D.

Figure 2 shows scaffolds of this general type, in a variety of geometric configurations to illustrate the design flexibility. Figure 2a and b highlights finite element analysis (FEA; see Methods for details) and an optical image of a representative 3D electronic scaffold that incorporates various microelectrodes (four electrodes for sensing and stimulation, one electrode for drug release, and one electrode as reference) at different height levels. In addition to controlling the spatial distribution of the electrodes, the assembly technique can also tailor precisely the lateral dimensions and heights of various features across the scaffold. For instance, the examples in Figure 2a and b have heights of ~ 770 μm in the central region for the development of engineered tissues.^{31,32} The 3D geometries predicted by FEA (Figure 2a, Figure S4 and Movie S2 in the Supporting Information) exhibit excellent agreement with measured results (Figure 2b), thereby establishing FEA as a reliable tool for guiding the selection of 2D precursors for desired 3D structural designs. Electrochemical measurements in

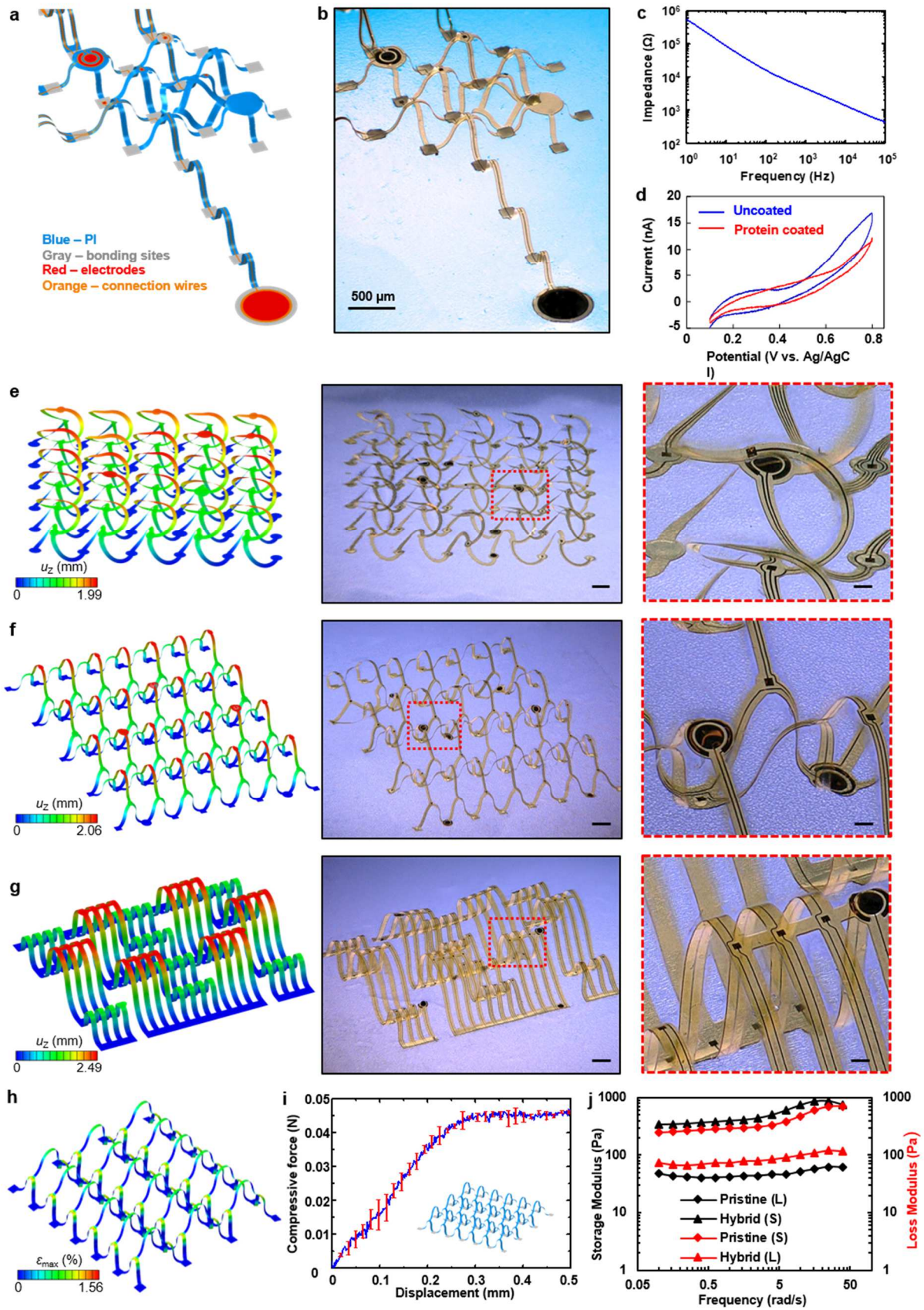


Figure 2. Various 3D electronic tissue scaffolds formed by mechanically-guided assembly. (a) Finite element modeling of a 3D electronic scaffold with electrodes and connection wires. (b) Optical image of the 3D electronic scaffold. (c) Impedance characterization of electrodes evaluated in cell culture medium. (d) Ferrocyanide/Ferricyanide oxidation tests of the

electrodes before and after protein treatment. (e-g) Optical images and FEA modeling of various 3D electronic scaffolds. Scale bar for (b), 500 μm . Scale bars for (e-g), 1 mm for the middle column images, and 200 μm for the right column images. (h) The maximum principal strain contour of the 3D tissue scaffold after the contraction of the cardiac tissue and hydrogel complex based on FEA. (i) DMA measurement of the 3D electronic scaffold. (j) Rheological measurement of the pristine hydrogel and the hybrid 3D electronic scaffold. “S” represents “Storage”, and “L” represents “Loss”.

Figure 2c indicate low impedance values across a relevant range of frequencies for electrodes in cell culture media at room temperature, which are comparable to those of commonly used electrode materials for measuring cardiac electrical activities to yield a high signal-to-noise ratio.³³⁻³⁵ Cyclic voltammetry curves in Figure 2d demonstrate that the electrodes are electrochemically active, as evidenced by the oxidation waves measured within a ferri/ferrocyanide solution. A comparison between measurements performed before and after coating the device with fibronectin, to promote cell adhesion, suggests that the adsorbed protein does not block the activity of these electrodes.

Figure 2e-g and Figure S5-S7 (Supporting Information) highlight additional 3D electronic scaffolds in other complex layouts, with increased numbers of electrodes and diversity of locations. The example of a double-floor helical architecture (Figure 2e and Figure S5, Supporting Information) includes 59 independently addressable electrodes, with 51 of these for electrical sensing and stimulation, 6 for drug release electrodes, and 2 reference electrodes. The microscale square electrodes for sensing and stimulation are uniformly distributed at three height levels above the substrate (0 mm, 1 mm, and 2 mm), corresponding to the bonding site, the midspan of the first-floor helices, and the midspan of the second-floor helices. The circular electrodes are located at both the edge and the center of the scaffold at three height levels for electrical stimulation and release of biofactors to the engineered tissue at various spatial locations. With a similar geometric layout as the scaffold in Figure 1, the design in Figure 2f and S6 (Supporting Information) has 56 electrodes (48 sensing and stimulation electrodes, 6

drug release electrodes, and 2 reference electrodes). The 3D ‘archway’ electronic scaffold in Figure 2g and Figure S7 (Supporting Information) has a collection of 86 electrodes (78 sensing and stimulation electrodes, 6 drug release electrodes, and 2 reference electrodes) distributed in clusters. Layouts for electrodes within the 3D electronic scaffold and an electronic scaffold with built-in ACF cables are shown in Figure S5-S10 (Supporting Information). The precisely-determined electrode distribution can potentially allow spatial-temporal controlled sequential activation of cardiac myocyte-tissue via ordered stimulation. In addition, other capabilities including temperature^{15,36} and pH³⁷ sensing can be integrated in a straightforward manner.

Mechanical integrity, with a sufficient level of mechanical compliance, is important in providing robust structural support without imposing significant constraints to natural motions of soft biological tissues^{38,39}, where, as an example, cardiomyocytes and cardiac tissues typically contract ~10% of their original size.^{40,41} To evaluate the mechanical integrity and compliance of the 3D electronic scaffolds under tissue contraction, we performed FEA simulations and experimental characterizations of 3D electronic scaffolds. Using FEA, we applied ~10% biaxial contraction to a mixture of cardiac tissue and ECM-based hydrogel integrated with the 3D electronic scaffold (Figure S11, Methods, Supporting Information). The results show that the scaffold exhibits a maximum principal strain of ~1.56% after tissue contraction (~5% increase compared with that in the as-fabricated 3D scaffold), which is well below the failure strain of the scaffold materials^{42,43} and indicates sufficient mechanical integrity (Figure 2h and Figure S12, Supporting Information). In addition, the scaffold deforms compliantly with the soft cardiac tissue, showing 5.4% longitudinal contraction of its original size (based on FEA results). We also performed mechanical characterization of 3D electronic scaffolds via dynamic mechanical analysis (DMA), as shown in Figure 2i. The 3D electronic scaffold exhibits much smaller modulus (493 Pa) than that of cardiac tissues and hydrogel scaffolds (18±2kPa).⁴⁴⁻⁴⁷ Such good mechanical compliance of 3D electronic scaffolds is

mainly attributed to the thin (6 μm thick) and narrow (130 μm wide) geometries of its ribbon components, and the resulting ultralow bending stiffness ($\sim 6 \times 10^{-12} \text{ N}\cdot\text{m}^2$), which can be further optimized through selection of the materials and structural geometries. To evaluate the impact of 3D electronics on the viscoelastic properties of the hybrid 3D electronic-hydrogel scaffold (to be discussed later), we performed rheological measurements of the pristine hydrogel used in this work and the hybrid 3D electronic scaffold. Figure 2j and Figure S13 (Supporting Information) show that the integration of 3D electronics within the hydrogel does not significantly alter its viscoelastic properties. Such mechanical and viscoelastic attributes make these 3D electronic scaffolds well suited for probing the physicochemical tissue microenvironment throughout their 3D and macroporous interior.

2.2 Controlled drug release from 3D electronic scaffolds

We first demonstrate the capability of controlled drug release from the fabricated 3D electronic scaffolds through the release of the anti-inflammatory drug dexamethasone (DEX). One of the major challenges in tissue engineering is reducing the immune reaction following transplantation.⁴⁸ Previous work demonstrates the potential of polypyrrole, an electroactive polymer that can be deposited onto conductive surfaces by electropolymerization through oxidation, for the controlled release of negatively charged drugs.^{17,18} By oxidation of the pyrrole monomer in the presence of a negatively charged molecule, a positively charged polymer film is deposited onto the electrode with negatively charged molecules trapped within its matrix through electrostatic bonds to the polymer backbone. Reduction of the polymer film through the same electrode leads to disruption of the electrostatic bonds and release of the negatively charged molecules (**Figure 3a**).

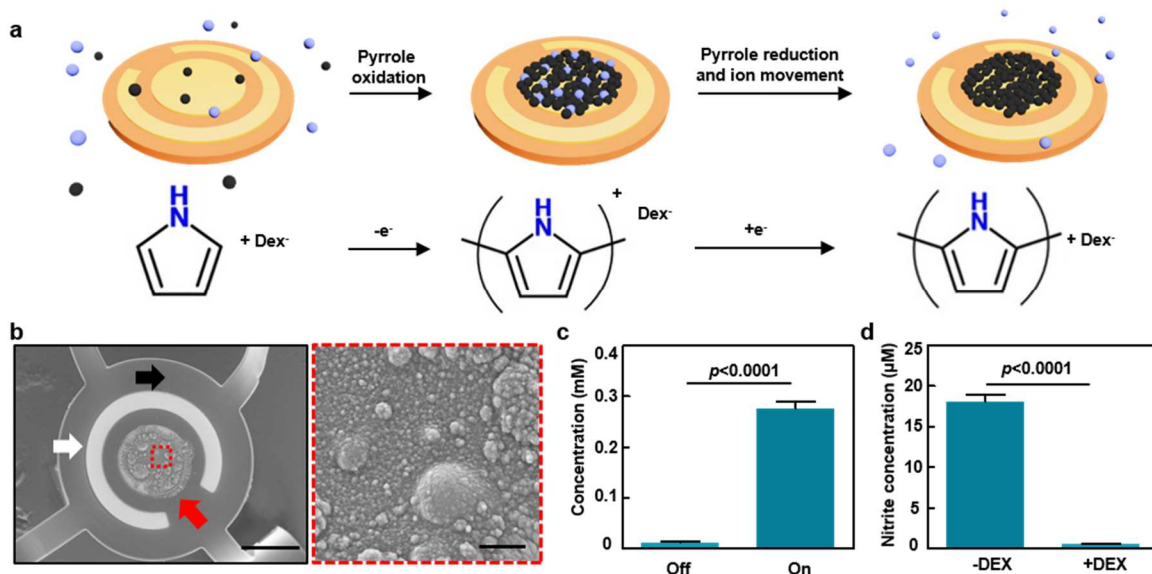


Figure 3. Controlled drug release from the 3D electronic scaffold. (a) Schematic representation of a system designed to release negatively charged drugs. The pyrrole monomers (black circles) are oxidized, leading to the creation of a PPy film containing the negatively charged drug (blue circles). On PPy reduction, the electrostatic bonds between the polymer and the drugs are broken, leading to the release of the drug. (b) Scanning electron micrograph of a polypyrrole film deposited upon an electrode in the 3D electronic scaffold (scale bar, 200 μm) and zoom in of the polypyrrole film (scale bar, 20 μm). Black arrow indicates the polyimide structure, white arrow indicates the surrounding counter electrode and the red arrow indicates the polypyrrole covered working electrode. (c) Dexamethasone release from within the deposited polypyrrole film. (d) Immune cell function as measured by NO secretion (measured as nitrite, a stable metabolite of NO) from activated macrophages, as a response to the DEX released from the device. All error bars represent the standard deviation ($n \geq 3$).

Dexamethasone (DEX) is a steroidal, anti-inflammatory drug commonly used following the implantation of biomedical devices to decrease the chances of immune rejection.⁴⁹ For example, anti-inflammatory DEX eluting cardiac pacemaker leads are used to decrease the inflammatory response following implantation.⁵⁰ Here, we use a derivative of DEX (dexamethasone 21-phosphate), which is negatively charged in physiological pH, and thus can be used as an anion in the electropolymerization process.

By applying a constant voltage of 1 V between the large electrode and its surrounding counter electrode, a layer of polypyrrole loaded with DEX was deposited on the large inner electrode of the 3D electronic scaffold (Figure 3b). The drug-loaded polymer formed a continuous film

covering the entire exposed electrode pad. It has been previously shown that, by increasing the amount of charge delivered in the electropolymerization process, polymer volume and concomitantly the amount of loaded drug can be increased.^{18,51} By reducing the polypyrrole film on the electrode, release of DEX (Figure 3c) was achieved. The application of a relatively weak electric field helps minimize the potential damage to the surrounding cells and the metal electrode itself, as has been demonstrated before.⁵² To evaluate the anti-inflammatory activity of the released DEX, it was added to a culture of macrophages following their activation with bacterial lipopolysaccharide. The released DEX significantly reduced the amount of secreted nitric oxide (NO), an indicator of macrophage inflammatory activity (Figure 3d).⁵³ By releasing anti-inflammatory agents into the surroundings of the implanted device, it is possible to reduce the amount of inflammation and increase the chances of graft survival. In order to evaluate the system's capability to release drugs over a longer time period, we performed on demand release of a second small anti-inflammatory molecule - acetylsalicylic acid, from the polypyrrole film on the device over a period of 5 days in three separate bursts. During this period, there was no significant drug release without the delivery of an electrical current. When desired, acetylsalicylic acid was released from the polypyrrole film in controlled bursts (Figure S14, supporting information). This ability to release drugs in a controlled manner over time could reduce the need for multiple invasive surgeries by reducing the damage from an inflammatory response and prolonging the effect of the treatment. As the formation of the polymer film is dependent upon the availability of a negatively charged small molecule, other useful small molecules, such as heparin, amiodarone, glutamate and indomethacin could potentially be loaded into the film and used to improve the outcome of the implantation. Recent work has shown that it is possible to release a variety of small molecules in an on/off profile using the polypyrrole system described here, and that by controlling the injected current and its duration it is possible to control the amount of released drug.²¹ The type of drug loaded into the system could be tailored according to the type of engineered tissue or organ. For example,

antihypertensive drugs could be released from within an engineered kidney to help modulate blood pressure and an engineered colon to potentially control nutrient absorption according to the patient's dietary needs. Finally, a variety of growth factors could be released in an autocrine fashion to control the fate of the cells within the engineered tissue microenvironment.

2.3 Biomaterial deposition and integration

Cardiomyocytes reside within a 3D fibrous network mostly composed of collagen fibers. These fibers provide cells with mechanical support and physical cues that lead to proper cell alignment and muscle bundle formation. To demonstrate the capabilities of the 3D electronic scaffold, we engineered a functional cardiac tissue by seeding cardiac cells within the scaffold that mimics the natural ECM.^{48,54} Recently, we developed a thermoresponsive ECM-based hydrogel prepared from a decellularized omentum. This hydrogel is liquid in room temperature and solidifies into gel form when placed in physiological conditions.^{55,56} As the hydrogel is composed of a decellularized tissue, it has been shown to retain its biochemical composition, fibrous architecture and mechanical properties that support cardiac cell culture and tissue formation.^{55,56}

In order to integrate the 3D electronic scaffold within the ECM-based hydrogel, we drop-casted the hydrogel, containing 1% ECM, in its liquid form onto the device. The liquid hydrogel does not damage the 3D architecture of the scaffold and can easily, entirely surround the 3D architecture from all directions forming a continuous matrix. After the hydrogel was allowed to solidify for 30 minutes in 37°C, a biomaterial-3D electronic hybrid scaffold was formed (**Figure 4a** and **b**). The degradation profiles of the hybrid and pristine scaffolds were monitored in physiological medium for 28 days. No significant difference was measured between them, which indicates that only the hydrogel component undergoes slow degradation in cell culture medium while the electronic component does not degrade (**Figure S15**, Supporting Information).

As the hydrogel is

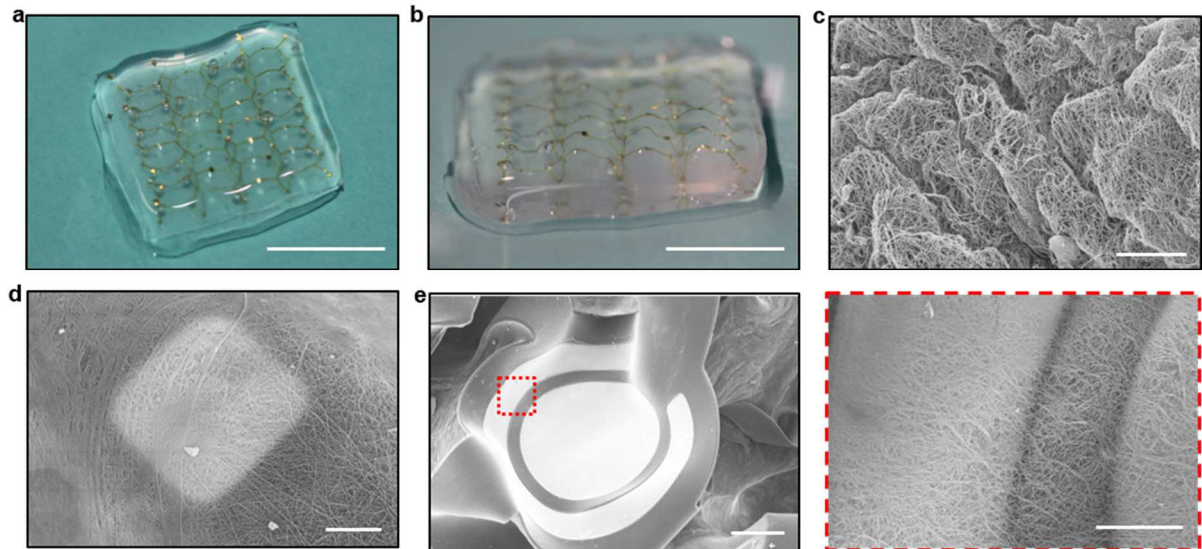


Figure 4. Biomaterial integration. (a-b) Optical images of the freestanding 3D electronic scaffold integrated within the ECM hydrogel. Scale bar, 1 cm. (c) Scanning electron micrograph of the ECM hydrogel. Scale bar, 10 μm . (d) Scanning electron micrograph of a small electrode embedded within the ECM hydrogel. Scale bar, 20 μm . (e) Scanning electron micrograph of a large electrode embedded within the ECM hydrogel (scale bar, 100 μm), and zoom in of the ECM hydrogel nanofibers covering the large electrode (scale bar, 20 μm).

predominantly composed of collagen and other ECM proteins, it will be degraded into smaller peptides by naturally occurring hydrolytic enzymes such as matrix metalloproteinases. The resulting degradation products can either be absorbed and recycled or may influence other physiological processes such as further collagen synthesis.^{57,58} Microcomputed tomography analysis of a simple 3D electronic scaffold embedded within the hydrogel showed no damage done to the 3D structural elements including delicate ribbons (Figure S16, Supporting Information). Scanning electron microscopy revealed that the hydrogel maintained its nanofibrous structure (Figure 4c) with an average fiber diameter of 123 ± 53 nm (Figure S17, Supporting Information). This fiber composition mimics that of the endomysial fibers in the natural cardiac ECM, which surround and support individual cardiomyocytes within the cardiac muscle.⁵⁴ These fibers connect to the plasma membrane using integrins to form connections between the ECM and the cytoskeleton proteins.⁵⁹ The resulting hydrogel fiber network is extremely permeable (with a solid content of 1%) and allows for cell penetration to the small

recording electrodes (Figure 4d). Drugs released from the electroactive polymers deposited onto the large stimulating electrodes can diffuse between the fibers and reach the cellular microenvironment. Concomitantly, due to the tight interaction between the hydrogel and the electrodes, potential delamination of the electroactive polymer layer is prevented (Figure 4e).

2.4 Tissue organization and function within the hybrid structures

Following the implantation of an engineered tissue, follow-up is focused on indirect data collection.⁴⁸ Through the integration of electronic systems within engineered tissues, it is possible to monitor the function of the engineered tissue from within, and control its fate by stimulation and biomolecule release.^{17,18,20}

To achieve proper contact with cells, surfaces are usually coated with adhesion promoting moieties such as laminin, fibronectin or polylysine.^{60,61} These species bind to the integrins in the cell membranes through specific amino acid sequences. Here, to induce proper integration within the engineered tissue, our 3D electronic scaffolds were pretreated with fibronectin, a protein containing the integrin binding, amino acid sequence arginine-glycine-aspartate.⁶² Cardiac cells were isolated from the left ventricles of neonatal rat hearts, mixed within the hydrogel and seeded onto the 3D electronic devices. In this manner, the liquid hydrogel can easily form a continuous matrix around and throughout the 3D architecture so that the cells can reach every location in the device. The in-vitro viability of the cardiac cells within pristine hydrogel and hybrid 3D electronic scaffolds were evaluated over 14 days by measuring their metabolic activity. The results show that the 3D electronics do not have any significant effect on the viability of the cardiac cells (Figure S18, Supporting Information). Ten days following cardiac cell seeding, the hybrid tissues were fixed and stained for α -sarcomeric actinin and DNA, a specific cardiac muscle marker. Confocal fluorescence microscopy images revealed elongated cardiomyocytes with a high aspect ratio (5.119 ± 0.1605), displaying striation (**Figure**

5a and b and Figure S19 and S20, Supporting Information). Additional staining for connexin 43, a protein associated with electrical coupling between adjacent cells⁶³, and visualization

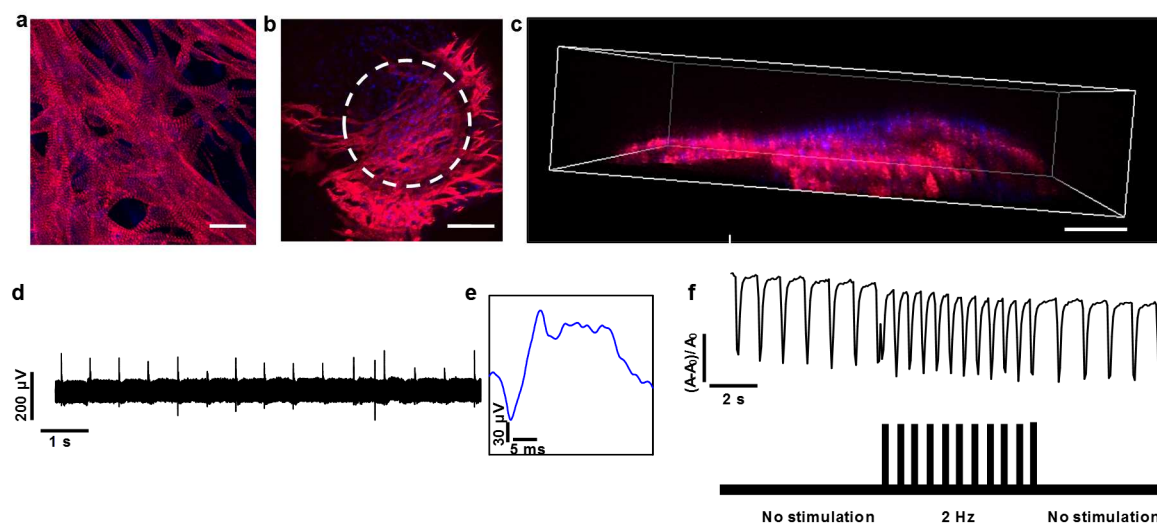


Figure 5. Tissue organization and function within the 3D electronic scaffold. (a) Zoomed-in image of cardiac cells showing cell elongation and striation. Sarcomeric actinin is in red, and nuclei are in blue (Hoechst 33258). Scale bar, 20 μm . (b) Confocal microscope image showing the assembled cardiac tissue within the hybrid device. Sarcomeric actinin is in red, and nuclei are in blue (Hoechst 33258). The borders of a circular stimulating electrode embedded within the cardiac tissue is highlighted with a dashed white circle. Scale bar, 100 μm . (c) 3D reconstruction of the cardiac tissue growing on top of the 3D electronic scaffold. Sarcomeric actinin-negative cells stain only in blue and most likely represent cardiac fibroblasts as well as other isolated non-myocyte cells. Scale bar, 100 μm . (d) Extracellular potential recordings from an electrode embedded within the cardiac tissue. (e) Magnified view of one representative recorded extracellular potential (f) Cardiac tissue contraction in response to an applied voltage (bottom) from within the 3D electronic scaffold.

of calcium transients demonstrated that the cells are electrically coupled and formed a spontaneously contracting confluent tissue with proper signal propagation (Figure S21 and Movie S3, Supporting Information). These indicate the mature state of the cells and the assembly of a cardiac tissue with native myocardial features.⁶⁴ Further inspection showed a close interaction between the cells and the 3D structure with cells growing on both the polyimide scaffolding and the exposed gold electrode pads (Figure 5b). Three-dimensional reconstruction images revealed cardiac tissue assembly in all dimensions, with organization along the architecture of the electronic scaffold (Figure 5c).

Once tissue assembly was established, the integrated electronics could be utilized to record electrophysiological data from within the engineered tissue. Recordings obtained from the small electrodes exhibited regularly spaced spikes with a frequency of up to 2 Hz and an amplitude of $\sim 200 \mu\text{V}$ (Figure 5d). The shape and width of the recorded signals are consistent with cardiomyocyte extracellular signals (Figure 5e).⁶⁵ Recordings from two separate electrodes allowed the estimation of the conduction velocity at $\sim 8 \text{ cm/s}$ (Figure S22, Supporting Information). Brightfield microscopy video captures of tissue contraction were taken at the same time as the gathered electrophysiological data in order to validate the reliability of the recorded extracellular signals (Movie S4, Supporting Information). Once recording of extracellular potentials within the tissue was achieved, we sought to evaluate the 3D electronic scaffold's ability to control tissue function.

Achieving synchronized contractions and signal conduction throughout the cardiac tissue is an important goal in tissue engineering. By integrating electronics to create cyborg cardiac tissues, it is possible to provide proper electrical stimulation in a controlled manner. This feature allows activation of non-contracting cells, synchronization of tissue contraction throughout the patch, as well as pacing of the tissue in a healthy rhythm.^{17,18,48} Electrical stimulation was achieved by the generation of a local electric field between a large electrode and its surrounding circular counter electrode. By applying a 3 V, 50 ms long signal, it was possible to change the contraction frequency of a tissue that was spontaneously contracting to either 1 or 2 Hz (Figure 5f, Figure S23a and Movies S5 and S6, Supporting Information). This feature could also be used to either induce or correct contraction arrhythmias (Figure S23b and c and Movies S7 and S8, Supporting Information). These signals did not affect the integrity of the scaffold or its 3D architecture.⁶⁶⁻⁶⁹ These results demonstrate the ability of the 3D electronic device to both monitor and control cell and tissue function. Due to the modularity of the 3D electronic scaffold design, it is possible to place stimulation and recording electrodes throughout the engineered

tissue at designated locations, much like cardiac pacemaker leads are placed in varying locations to achieve different stimulation patterns according to the required treatment. Additionally, through the application of long-term systematic electrical stimulation, training of the developing tissue can be achieved, which can promote tissue maturation and function.⁷⁰ This feature can affect the function of the engineered tissue and aid in its integration with the treated heart.

3. Conclusion

The results presented here demonstrate that 3D electronic structures formed via mechanically guided assembly approaches are well suited for integration with engineered cardiac tissues for online monitoring and regulation of tissue function. These hybrid 3D electronics-tissue systems can measure electrical activities of the engineered tissue, as well as control over its function by providing electrical stimulation for pacing and controlled drug release. Future work based on these hybrid tissues has the potential to allow for control over tissue geometry using complex architectures, with 3D vascular networks and high-performance electronic and optoelectronic devices. Such types of active scaffolds will allow interaction and communication with live cells and tissues in 3D, with possible applications in drug screening in real 3D environments, as a model of natural physiological conditions.

Acknowledgements

The authors acknowledge the support from the U.S. Department of Energy, Office of Science, Basic Energy Sciences (# DE-FG02-07ER46471). Y.Z. acknowledges the support from the National Natural Science Foundation of China (grant nos. 11502129 and 11722217) and the Tsinghua National Laboratory for Information Science and Technology. Y.H. acknowledges the support from the NSF (grant nos. CMMI1400169, CMMI1534120 and CMMI1635443).

Received: ((will be filled in by the editorial staff))
Revised: ((will be filled in by the editorial staff))
Published online: ((will be filled in by the editorial staff))

References

- 1 Langer, R. & Tirrell, D. A. Designing materials for biology and medicine. *Nature* **428**, 487-492, doi:10.1038/nature02388 (2004).
- 2 Shafiee, A. & Atala, A. Tissue Engineering: Toward a New Era of Medicine. *Annu Rev Med* **68**, 29-40, doi:10.1146/annurev-med-102715-092331 (2017).
- 3 Berthiaume, F., Maguire, T. J. & Yarmush, M. L. Tissue Engineering and Regenerative Medicine: History, Progress, and Challenges. *Annu Rev Chem Biomol* **2**, 403-430, doi:10.1146/annurev-chembioeng-061010-114257 (2011).

- 4 Dvir, T. *et al.* Prevascularization of cardiac patch on the omentum improves its
therapeutic outcome. *P Natl Acad Sci USA* **106**, 14990-14995,
doi:10.1073/pnas.0812242106 (2009).
- 5 O'Brien, F. J. Biomaterials & scaffolds for tissue engineering. *Mater Today* **14**, 88-95,
doi:Doi 10.1016/S1369-7021(11)70058-X (2011).
- 6 Ringe, J. & Sittinger, M. REGENERATIVE MEDICINE Selecting the right biological
scaffold for tissue engineering. *Nat Rev Rheumatol* **10**, 388-389,
doi:10.1038/nrrheum.2014.79 (2014).
- 7 Obien, M. E. J., Deligkaris, K., Bullmann, T., Bakkum, D. J. & Frey, U. Revealing
neuronal function through microelectrode array recordings. *Front Neurosci-Switz* **8**,
doi:ARTN 42310.3389/fnins.2014.00423 (2015).
- 8 Jiang, Y. & Tian, B. J. N. R. M. Inorganic semiconductor biointerfaces. 1 (2018).
- 9 Viventi, J. *et al.* A Conformal, Bio-Interfaced Class of Silicon Electronics for
Mapping Cardiac Electrophysiology. *Sci Transl Med* **2**, doi:ARTN
24ra2210.1126/scitranslmed.3000738 (2010).
- 10 Kim, D. H. *et al.* Materials for multifunctional balloon catheters with capabilities in
cardiac electrophysiological mapping and ablation therapy. *Nat Mater* **10**, 316-323,
doi:10.1038/Nmat2971 (2011).
- 11 Timko, B. P. *et al.* Electrical Recording from Hearts with Flexible Nanowire Device
Arrays. *Nano Lett* **9**, 914-918, doi:10.1021/nl900096z (2009).
- 12 Cohen-Karni, T., Timko, B. P., Weiss, L. E. & Lieber, C. M. Flexible electrical
recording from cells using nanowire transistor arrays. *P Natl Acad Sci USA* **106**, 7309-
7313, doi:10.1073/pnas.0902752106 (2009).
- 13 Viventi, J. *et al.* Flexible, foldable, actively multiplexed, high-density electrode array
for mapping brain activity in vivo. *Nat Neurosci* **14**, 1599-U1138,
doi:10.1038/nn.2973 (2011).
- 14 Kim, D. H. *et al.* Epidermal Electronics. *Science* **333**, 838-843,
doi:10.1126/science.1206157 (2011).
- 15 Krishnan, S. R. *et al.* Epidermal electronics for noninvasive, wireless, quantitative
assessment of ventricular shunt function in patients with hydrocephalus. **10**, eaat8437
(2018).
- 16 Xu, J. *et al.* Highly stretchable polymer semiconductor films through the
nanoconfinement effect. *Science* **355**, 59-+, doi:10.1126/science.aah4496 (2017).
- 17 Feiner, R., Fleischer, S., Shapira, A., Kalish, O. & Dvir, T. Multifunctional degradable
electronic scaffolds for cardiac tissue engineering. *Journal of Controlled Release*
(2018).
- 18 Feiner, R. *et al.* Engineered hybrid cardiac patches with multifunctional electronics for
online monitoring and regulation of tissue function. *Nat Mater* **15**, 679 (2016).
- 19 Dai, X., Zhou, W., Gao, T., Liu, J. & Lieber, C. M. Three-dimensional mapping and
regulation of action potential propagation in nanoelectronics-innervated tissues.
Nature Nanotechnology (2016).
- 20 Tian, B. *et al.* Macroporous nanowire nanoelectronic scaffolds for synthetic tissues.
Nat Mater **11**, 986 (2012).
- 21 Feiner, R. *et al.* A Stretchable and Flexible Cardiac Tissue–Electronics Hybrid
Enabling Multiple Drug Release, Sensing, and Stimulation. 1805526 (2019).
- 22 Xu, S. *et al.* Assembly of micro/nanomaterials into complex, three-dimensional
architectures by compressive buckling. *Science* **347**, 154-159 (2015).
- 23 Wang, X. *et al.* Freestanding 3D Mesostructures, Functional Devices, and Shape -
Programmable Systems Based on Mechanically Induced Assembly with Shape
Memory Polymers. *Advanced Materials*, 1805615 (2018).

- 24 Kim, B. H. *et al.* Mechanically Guided Post - Assembly of 3D Electronic Systems. *Advanced Functional Materials*, 1803149 (2018).
- 25 Kim, B. H. *et al.* Three-Dimensional Silicon Electronic Systems Fabricated by Compressive Buckling Process. *ACS nano* **12**, 4164-4171 (2018).
- 26 Yan, Z. *et al.* Three-dimensional mesostructures as high-temperature growth templates, electronic cellular scaffolds, and self-propelled microrobots. *Proceedings of the National Academy of Sciences* **114**, E9455-E9464 (2017).
- 27 Yan, Z. *et al.* Controlled mechanical buckling for origami - inspired construction of 3D microstructures in advanced materials. *Advanced functional materials* **26**, 2629-2639 (2016).
- 28 Zhang, Y. *et al.* A mechanically driven form of Kirigami as a route to 3D mesostructures in micro/nanomembranes. *Proceedings of the National Academy of Sciences* **112**, 11757-11764 (2015).
- 29 Zhang, Y. H. *et al.* Printing, folding and assembly methods for forming 3D mesostructures in advanced materials (vol 2, pg 17019, 2017). *Nat Rev Mater* **2** (2017).
- 30 Fu, H. R. *et al.* Morphable 3D mesostructures and microelectronic devices by multistable buckling mechanics. *Nat Mater* **17**, 268+, doi:10.1038/s41563-017-0011-3 (2018).
- 31 Griffith, C. K. *et al.* Diffusion limits of an in vitro thick prevascularized tissue. *Tissue engineering* **11**, 257-266 (2005).
- 32 Zimmermann, W.-H. *et al.* Engineered heart tissue grafts improve systolic and diastolic function in infarcted rat hearts. *Nature medicine* **12**, 452-458 (2006).
- 33 Dai, X. C., Zhou, W., Gao, T., Liu, J. & Lieber, C. M. Three-dimensional mapping and regulation of action potential propagation in nanoelectronics-innervated tissues. *Nat Nanotechnol* **11**, 776-782, doi:10.1038/Nnano.2016.96 (2016).
- 34 Feiner, R. *et al.* Engineered hybrid cardiac patches with multifunctional electronics for online monitoring and regulation of tissue function. *Nat Mater* **15**, 679+, doi:10.1038/Nmat4590 (2016).
- 35 Xu, L. Z. *et al.* 3D multifunctional integumentary membranes for spatiotemporal cardiac measurements and stimulation across the entire epicardium. *Nat Commun* **5**, doi:ARTN 332910.1038/ncomms4329 (2014).
- 36 Gao, W., Ota, H., Kiriya, D., Takei, K. & Javey, A. J. A. o. c. r. Flexible Electronics toward Wearable Sensing. (2019).
- 37 Chung, H. J. *et al.* Stretchable, multiplexed pH sensors with demonstrations on rabbit and human hearts undergoing ischemia. **3**, 59-68 (2014).
- 38 Sim, K. *et al.* Fully rubbery integrated electronics from high effective mobility intrinsically stretchable semiconductors. **5**, eaav5749 (2019).
- 39 Bolaños Quiñones, V. A., Zhu, H., Solovev, A. A., Mei, Y. & Gracias, D. H. J. A. B. Origami Biosystems: 3D Assembly Methods for Biomedical Applications. **2**, 1800230 (2018).
- 40 Yaniv, Y. *et al.* Analysis of Mitochondrial 3D-Deformation in Cardiomyocytes during Active Contraction Reveals Passive Structural Anisotropy of Orthogonal Short Axes. *Plos One* **6**, doi:ARTN e2198510.1371/journal.pone.0021985 (2011).
- 41 Carlsson, M. *et al.* Total heart volume variation throughout the cardiac cycle in man. (2004).
- 42 Jang, K. I. *et al.* Soft network composite materials with deterministic and bio-inspired designs. *Nat Commun* **6**, doi:ARTN 656610.1038/ncomms7566 (2015).
- 43 Hong, H. C. & Chen, C. M. Design, Fabrication and Failure Analysis of Stretchable Electrical Routings. *Sensors-Basel* **14**, 11855-11877, doi:10.3390/s140711855 (2014).

- 44 Ramadan, S., Paul, N. & Naguib, H. E. Standardized static and dynamic evaluation of myocardial tissue properties. *Biomed Mater* **12**, doi:ARTN 02501310.1088/1748-605X/aa57a5 (2017).
- 45 Hiesinger, W. *et al.* Myocardial tissue elastic properties determined by atomic force microscopy after stromal cell-derived factor 1 α angiogenic therapy for acute myocardial infarction in a murine model. **143**, 962-966 (2012).
- 46 Ahearne, M., Yang, Y. & Liu, K. J. T. i. t. E. Mechanical characterisation of hydrogels for tissue engineering applications. **4**, 1-16 (2008).
- 47 Czerner, M., Fellay, L. S., Suarez, M. P., Frontini, P. M. & Fasce, L. A. Determination of Elastic Modulus of Gelatin Gels by Indentation Experiments. *Proc Mat Sci* **8**, 287-296, doi:10.1016/j.mspro.2015.04.075 (2015).
- 48 Fleischer, S., Feiner, R. & Dvir, T. Cutting-edge platforms in cardiac tissue engineering. *Current opinion in biotechnology* **47**, 23-29 (2017).
- 49 Tsurufuji, S., Sugio, K. & Takemasa, F. The role of glucocorticoid receptor and gene expression in the anti-inflammatory action of dexamethasone. *Nature* **280**, 408 (1979).
- 50 Tomaske, M. *et al.* A 12-year experience of bipolar steroid-eluting epicardial pacing leads in children. *The Annals of Thoracic Surgery* **85**, 1704-1711 (2008).
- 51 Wadhwa, R., Lagenaur, C. F. & Cui, X. T. Electrochemically controlled release of dexamethasone from conducting polymer polypyrrole coated electrode. *Journal of controlled release* **110**, 531-541 (2006).
- 52 Feiner, R. *et al.* Engineered hybrid cardiac patches with multifunctional electronics for online monitoring and regulation of tissue function. *Nature materials* (2016).
- 53 Kim, J.-H. *et al.* Sulfated chitosan oligosaccharides suppress LPS-induced NO production via JNK and NF- κ B inactivation. *Molecules* **19**, 18232-18247 (2014).
- 54 Fleischer, S. & Dvir, T. Tissue engineering on the nanoscale: lessons from the heart. *Current opinion in biotechnology* **24**, 664-671 (2013).
- 55 Shevach, M. *et al.* Omentum ECM-based hydrogel as a platform for cardiac cell delivery. *Biomedical Materials* **10**, 034106 (2015).
- 56 Edri, R. *et al.* Personalized Hydrogels for Engineering Diverse Fully Autologous Tissue Implants. *Advanced Materials*, 1803895 (2018).
- 57 Gardi, C. *et al.* Collagen breakdown products and lung collagen metabolism: an in vitro study on fibroblast cultures. *Thorax* **49**, 312-318 (1994).
- 58 Bejarano, P. A., Noelken, M. E., Suzuki, K., Hudson, B. & Nagase, H. Degradation of basement membranes by human matrix metalloproteinase 3 (stromelysin). *Biochemical Journal* **256**, 413-419 (1988).
- 59 Pope, A. J., Sands, G. B., Smaill, B. H. & LeGrice, I. J. Three-dimensional transmural organization of perimysial collagen in the heart. *American Journal of Physiology-Heart and Circulatory Physiology* **295**, H1243-H1252 (2008).
- 60 Mazia, D., Schatten, G. & Sale, W. Adhesion of cells to surfaces coated with polylysine. Applications to electron microscopy. *The Journal of cell biology* **66**, 198-200 (1975).
- 61 Dean III, J. W., Culbertson, K. C. & D'Angelo, A. M. Fibronectin and laminin enhance gingival cell attachment to dental implant surfaces in vitro. *International Journal of Oral & Maxillofacial Implants* **10** (1995).
- 62 Mao, Y. & Schwarzbauer, J. E. Fibronectin fibrillogenesis, a cell-mediated matrix assembly process. *Matrix biology* **24**, 389-399 (2005).
- 63 You, J.-O., Rafat, M., Ye, G. J. & Auguste, D. T. Nanoengineering the heart: conductive scaffolds enhance connexin 43 expression. *Nano letters* **11**, 3643-3648 (2011).
- 64 Zimmermann, W.-H. *et al.* Tissue engineering of a differentiated cardiac muscle construct. *Circulation research* **90**, 223-230 (2002).

- 65 Bursac, N. *et al.* Cardiac muscle tissue engineering: toward an in vitro model for electrophysiological studies. *American Journal of Physiology-Heart and Circulatory Physiology* **277**, H433-H444 (1999).
- 66 Dvir, T., Timko, B. P., Kohane, D. S. & Langer, R. Nanotechnological strategies for engineering complex tissues. *Nature nanotechnology* **6**, 13-22 (2011).
- 67 Li, M., Guo, Y., Wei, Y., MacDiarmid, A. G. & Lelkes, P. I. Electrospinning polyaniline-contained gelatin nanofibers for tissue engineering applications. *Biomaterials* **27**, 2705-2715 (2006).
- 68 Kai, D., Prabhakaran, M. P., Jin, G. & Ramakrishna, S. Polypyrrole - contained electrospun conductive nanofibrous membranes for cardiac tissue engineering. *Journal of Biomedical Materials Research Part A* **99**, 376-385 (2011).
- 69 Roshanbinfar, K. *et al.* Electroconductive biohybrid hydrogel for enhanced maturation and beating properties of engineered cardiac tissues. *Advanced Functional Materials* **28**, 1803951 (2018).
- 70 Ronaldson-Bouchard, K. *et al.* Advanced maturation of human cardiac tissue grown from pluripotent stem cells. *Nature* **556**, 239 (2018).

The table of contents entry

This paper presents the development of 3D porous, flexible electronic scaffolds with well-defined microelectrode distributions and their integration with engineered cardiac tissues for the sensing, stimulation and regulation of tissue function. The resulting engineering options provide opportunities in fields ranging from in vitro drug development to in vivo tissue repair and many others.

Keyword: 3D electronic scaffolds, cardiac tissue engineering, electronic stimulation, drug release, mechanically-guided assembly

Xueju Wang[†], Ron Feiner[†], Haiwen Luan[†], Qihui Zhang, Shiwei Zhao, Yi Zhang, Mengdi Han, Yi Li, Rujie Sun, Heling Wang, Tzu-Li Liu, Xiaogang Guo, Hadas Oved, Nadav Noor, Assaf Shapira, Yihui Zhang, Yonggang Huang*, Tal Dvir*, and John A. Rogers*

Title: Three-Dimensional Electronic Scaffolds for Monitoring and Regulation of Multifunctional Hybrid Tissues

ToC figure

